Experimental study on wave forces to offshore support structures

Youn-Ju Jeong[*], Min-Su Park[a] and Young-Jun You[b]

*Structural Engineering Research Institute, Korea Institute of Civil Engineering and Building Technology,
283 Goyangdae-ro, ilsanseo-gu, Goyang, Gyeonggi 10223, Republic of Korea*

Abstract.   In this study, wave force tests were carried out for the four types of offshore support structures with scale factor 1:25 and wave forces to the support structure shapes were investigated. As the results of this study, it was found that, as the wave period increased at the normal wave condition, wave force decreased for the most cases. Extreme wave force was affected by the impact wave force. Impact wave force of this study significantly effect on Monopile and slightly on GBS and Hybrid type. Accordingly, Hybrid type indicated even lower wave force at the extreme and irregular wave conditions than the Monopile although Hybrid type indicated higher wave force at the normal wave condition of the regular wave because of the larger wave area of wave body. In respects of the structural design, since critical loading is extreme wave force, it should be contributed to improve structural safety of offshore support structure. However, since the impact wave force has nonlinearity and complication dependent on the support structure shape, wave height, wave period, and etc., more research is needed to access the impact wave force for other support structure shapes and wave conditions.

Keywords: offshore; support structure; shape; wave force test; impact wave force; extreme wave

1. Introduction

Offshore support structures should have a structural safety against to the harsh offshore conditions of wind, wave, and tidal. In order to improve structural safety of offshore support structure, it is important to reduce wave force and wave-induced bending moment to the support structure (Park *et al.* 2010, 2012). Most of the recent offshore support structures for wind turbine are monopile, jacket, and GBS (Gravity Based Structures). Recently, in order to improve wind energy availability and economic efficiency, the capacity of wind turbine is drastically increasing. According to the increasing of offshore wind turbine capacity, support structure also should be large-sized. However, the increasing of the size of support structure to improve strength and stiffness disadvantages to the wave forces subjected to the support structures because of the larger cross-sectional area of wave body. Therefore, it needs to optimally arrange structural components

---

*Corresponding author, Ph.D., E-mail: yjjeong@kict.re.kr
[a]Ph.D., E-mail: mspark@kict.re.kr
[b]Ph.D., E-mail: yjyou@kict.re.kr

(a) NEDO (Japan)   (b) Rockmat Ltd (France)   (c) KICT (South Korea)
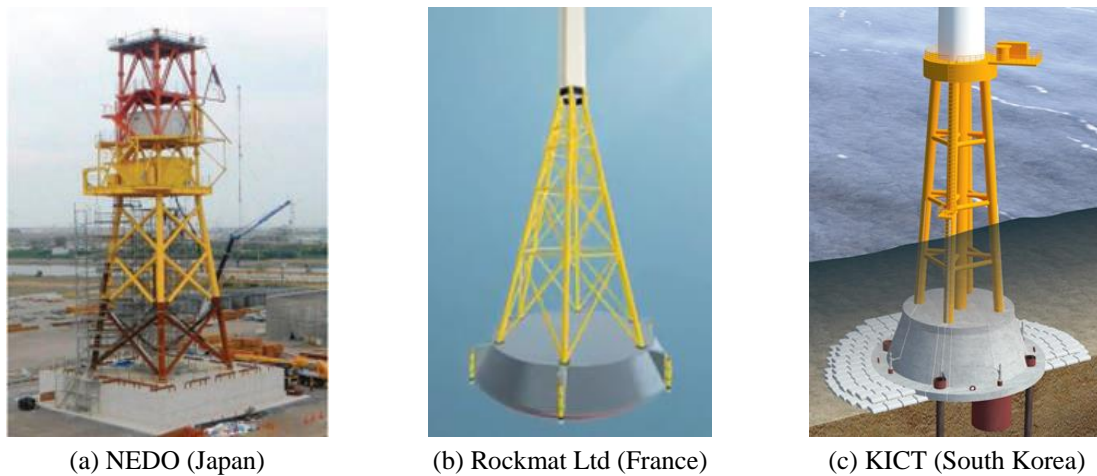
Fig. 1 Jacket-GBS hybrid support structures

of support structure so as to satisfy both low-wave force and high-structural safety (Jeong *et al*. 2015)

In this respects, hybrid types of support structures have been developed in Japan (NEDO 2013), France (Rockmat 2013), and South Korea (Jeong *et al*. 2013, 2014), etc. In Japan, NEDO (New Energy and Industrial Technology Development Organization) has been developed hybrid gravity type of support structure system. This type was designed by adopting the advantages of the gravity and jacket system, as presented in Fig. 1(a), and reported to reduce overturning moment about 80 % compared to the typical gravity type. This type was constructed as offshore wind condition observation tower in June, 2012 (NEDO 2013). In France, Rockmat Ltd. also has been developed hybrid jacket type of support structure for the rocky seabed. This type was similar with the NEDO's hybrid gravity type, as presented in Fig. 1(b). This system adopted flexible cofferdam bags system to easily flat uneven seabed by injection the concrete and to simply uninstall support structure after the service life. In South Korea, KICT (Korea Institute of Civil Engineering and Building Technology) has been developing hybrid support structure which was similar with the NEDO (Japan) and Rockmat (France) systems. This system adopted multipiles to reduce wave force to the support structure and partial suction system combining foundation piles to easily position in the clay seabed.

In respects of the structural design, in the hydrodynamic analysis and structural analysis, wave forces subjected to the support structure are calculated from Morison equation or diffraction theory according to the shapes or dimensions of support structures. However, it has known that these theoretical wave forces do not reflect wave run-up or impact wave force effect at the extreme wave condition (Christensen *et al*. 2005, De Vos *et al*. 2007, Chella *et al*. 2012). Therefore, for the structural design of the offshore support structures, impact wave forces at the extreme wave condition has been evaluated experimentally within a certain structural shape and design wave condition of the wave height and wave period because of the nonlinearity and complication of the impact wave force (Christensen *et al*. 2005, De Vos *et al*. 2007, Chella *et al*. 2012, Cao *et al*. 2016).

In this study, in order to investigate wave force to the shapes of support structures, wave force tests were carried out for the four types of offshore support structures, Monopile (Fischer *et al*.
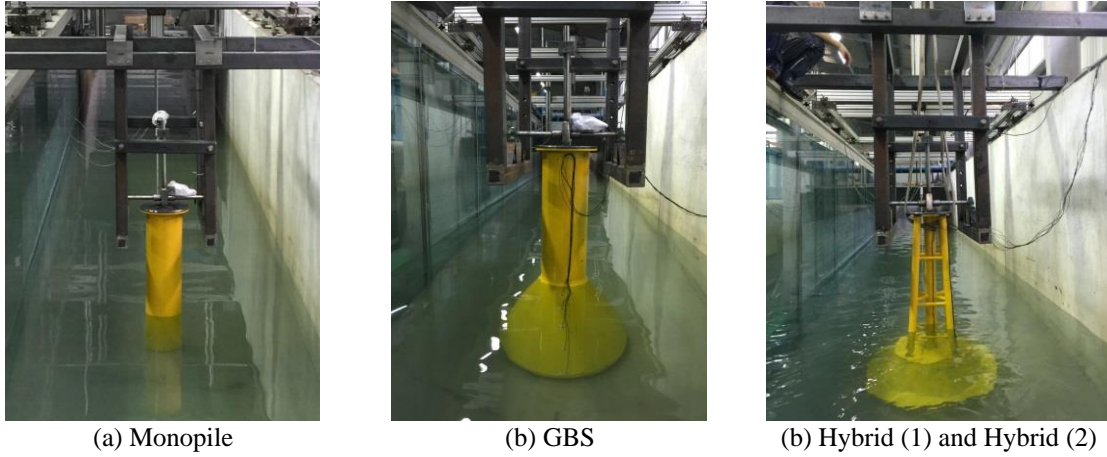
| (a) Monopile | (b) GBS | (b) Hybrid (1) and Hybrid (2) |

Fig. 2 Test models

Fig. 3 Area and volume of wave body

2010), GBS (Brook-Hart *et al*. 2010, Park *et al*. 2015), Hybrid (1), and Hybrid (2) types (Jeong *et al*. 2013, 2014). Based on the wave force tests, wave forces to the shapes of the support structures were analyzed and compared with each other.

2. Wave force tests

2.1 Test models

In order to evaluate wave force subjected to the offshore support structures, four types of support structures of Monopile, GBS, Hybrid (1), and Hybrid (2) were fabricated and tested under the various wave conditions, as presented in Fig. 2. Four types of support structures were designed and fabricated with the Froude scale law of 1:25. Three types of test models of Monopile, GBS, and Hybrid (1) had the same total weight and height. Hybrid (1) and Hybrid (2) had the same dimension but different weight of the bottom base part. Hybrid (1) and Hybrid (2) types were fabricated connecting multipiles of the upper part with the base of the bottom part. Therefore, Hybrid (1) and Hybrid (2) types had the same upper multipiles and different bottom base model which different in weight. The wave area ratios, as presented in Fig. 3, of GBS, Hybrid (1), and Hybrid (2) models to Monopile were about 2.1, 1.8, and 1.8, respectively, and wave volume ratios,

Table 1 Details of test models

No.	Type	Dimension (mm)	Weight (kg)	Wave area (cm^2)	Wave volume (cm^3)	Scale
1	Monopile	240(D_1)×240 D_2)×1,500(H)	203.00	1,920.0 (1.0)	11,520.0 (1.0)	1:25
2	GBS	260(D_1)×740(D_2)×1,500(H)	203.00	4,000.0 (2.1)	50,000.0 (4.3)	1:25
3	Hybrid(1)	272(D_1)×740(D_2)×1,500(H)	203.00	3,462.4 (1.8)	38,863.1 (3.4)	1:25
4	Hybrid(2)	*** D_1=(4·Ø 48+Ø 80)***	248.29	3,462.4 (1.8)	38,863.1 (3.4)	1:25

* D_1: top diameter, D_2: bottom diameter, H: height
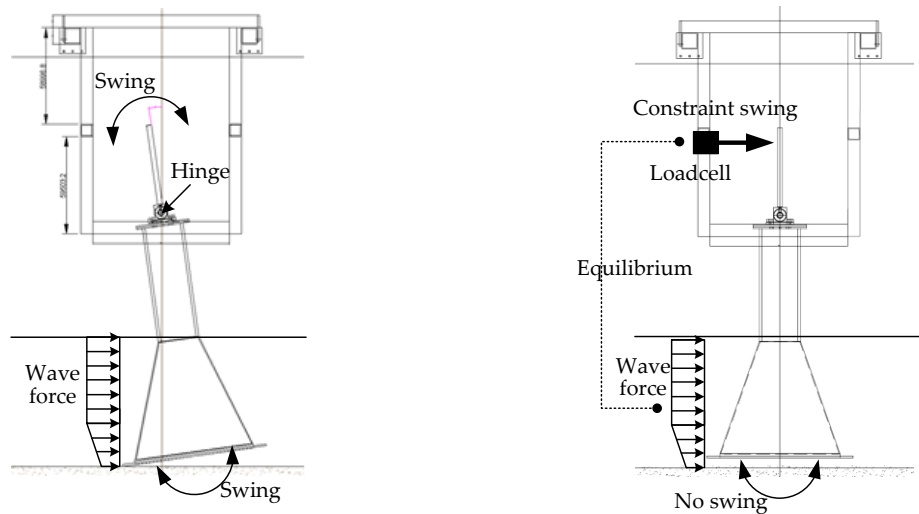
Fig. 4 Concept of wave force measurement

as presented in Fig. 3, were about 4.3, 3.4, and 3.4, respectively. In Fig. 3, D and H were the diameter and height of the structural member, respectively, as described in Table 1. The details of four support models were summarized in Table 1.

2.2 Test setup

In order to investigate wave force subjected to the support structures, experimental studies were conducted at the flume of the Cheonnam National University (local campus at Yeusu) of the South Korea in July, 2015. The dimensions of the flume were 100 m (L)×2.0 m (W)×3.0 m (H). The mechanical frame was specially designed and fabricated to allow wave-induced swing motion of test models with the minimum friction, as presented in Fig. 4 and Fig. 5(a). Then, some device to constraint wave-induced swing motions of test models, which connected with the load-cell, was attached to the mechanical frame, as presented in Fig. 5(a). Then, the loads to constraint swing motion of test models were measured using the load-cell. Constraint force was equal to the wave force subjected to the test models because test models maintained equilibrium to the swing motion. This test method had an advantage to remove sensor malfunction and error in the seawater since load-cell was positioned in the air. In order to measure wave pressure distribution along to the water depth, five to eight hydraulic pressure gauges were attached to the front side of the test models, as presented in Fig. 5(b).
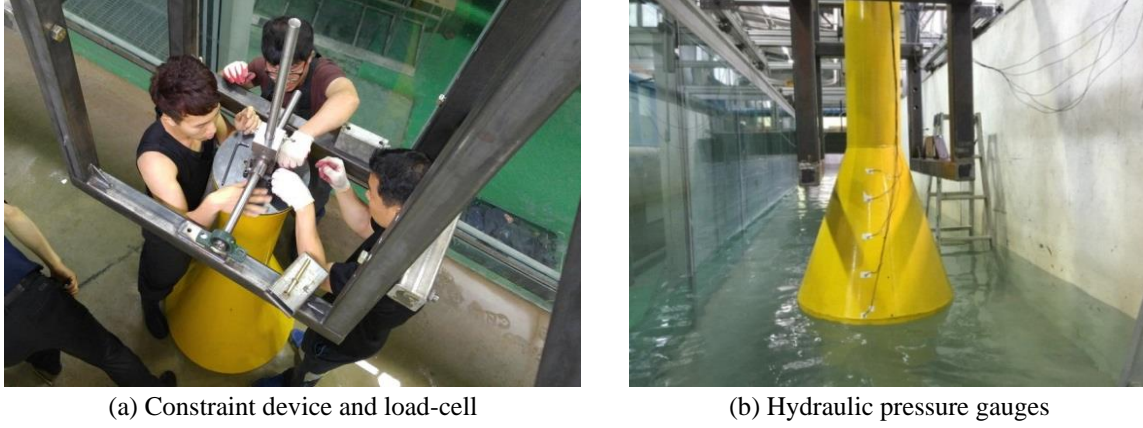
(a) Constraint device and load-cell (b) Hydraulic pressure gauges

Fig. 5 Installation of the sensors

Table 2 Wave conditions

Sea state		No.	Wave height H_w (m)	Wave period P_w (s)	Wave length L_w (m)	H_w/L_w
Regular	Normal	#1	0.137 (3.435)	1.50 (7.5)	3.217 (80.429)	1/23.41
		#2	0.137 (3.435)	1.90 (9.5)	4.530 (113.269)	1/32.97
		#3	0.137 (3.435)	2.30 (11.5)	5.787 (144.674)	1/42.11
		#4	0.137 (3.435)	2.74 (13.5)	7.124 (178.122)	1/51.85
		#5	0.137 (3.435)	3.10 (15.5)	8.197 (204.940)	1/59.66
	Extreme	#6	0.511 (12.78)	2.74 (13.5)	7.124 (178.122)	1/13.94
Irregular		#7	0.137 (3.435)	1.50 (7.5)	3.217 (80.429)	1/23.41
		#8	0.137 (3.435)	1.90 (9.5)	4.530 (113.269)	1/32.97
		#9	0.137 (3.435)	2.30 (11.5)	5.787 (144.674)	1/42.11
		#10	0.275 (6.870)	2.75 (13.7)	7.124 (178.122)	1/25.97

* (　) outside: small-scale model, (　) inside: full-scale model

2.3 Wave conditions

Support structure models were tested under the six regular wave and four irregular wave conditions, as presented in Table 2 and Fig. 6. The wave variables of this wave test were the wave height and wave period. For the full-scale models on the regular wave, two cases of wave height (H_w) 3.435 m and 12.78 m were selected and these were scale downed to 0.137 m and 0.511 m by Froude scale law of $1/\lambda$, where λ was a scale factor, for the small-scale model. Also, for the wave height 3.435 m, five cases of wave period (P_w) 7.5 s, 9.5 s. 11.5 s, 13.5 s, and 15.5 s were selected and these were scale downed to 1.5 s, 1.9 s, 2.3 s, 2.74 s, and 3.1 s by Froude scale low of $1/\sqrt{\lambda}$ for the small-scale model. Wave length was calculated by wave theory of Eq. (1).

$$L_w = \frac{gP_w{}^2}{2\pi} \tanh(\frac{2\pi h}{L_w}) \tag{1}$$

where, P_w and L_w are the wave period and wave length, respectively. g is the acceleration of

gravity (m/s^2) and h is the water depth (m), respectively. Among the six regular wave conditions of Table 2, wave #3 (wave height 3.435 m and wave period 11.5 s) was corresponded to the normal wave condition and wave #6 (wave height 12.78 m and wave period 13.5 s) was corresponded to the extreme wave condition at the structural design. Four irregular wave conditions were generated with JONSWAP spectrum. H_w/L_w ratios of ten wave conditions were set up to satisfy wave breaking requirement 1/7.14 (DNV 2013) to prevent wave breaking at the flume, as presented in Table 2. Water depth (*h*) was 20.0 m and scale downed to 0.8 m by the scale factor.

In cases of Hybrid (1) and Hybrid (2) models, incident wave 45° as well as 0° was added to verify maximum wave forces according to the incident wave effect, since the upper part of Hybrid (1) and Hybrid (2) models consist of the multiplies and indicated different wave force to the wave direction. In order to act incident wave 45° effect, Hybrid (1) and Hybrid (2) models were repositioned to the 45° direction for the wave direction. Wave force tests were carried out during the 300 s. Among the measured time series load-cell data, 50 s data from 200 s to 250 s was selected as the typical wave force, which was well presented wave force of test models. Noise of measured data set was eliminated using moving average data processing method. Based on the measured data, minimum and maximum magnitudes of the wave forces were calculated for the small-scale models and converted for the real-scale models according to the Froude scale law.
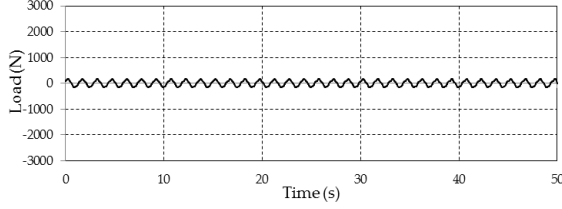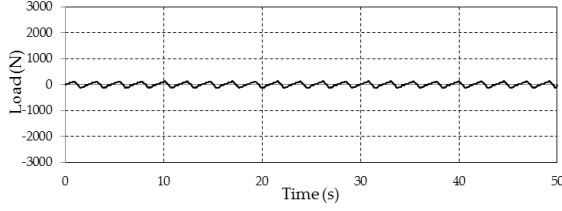

(a) Normal wave condition
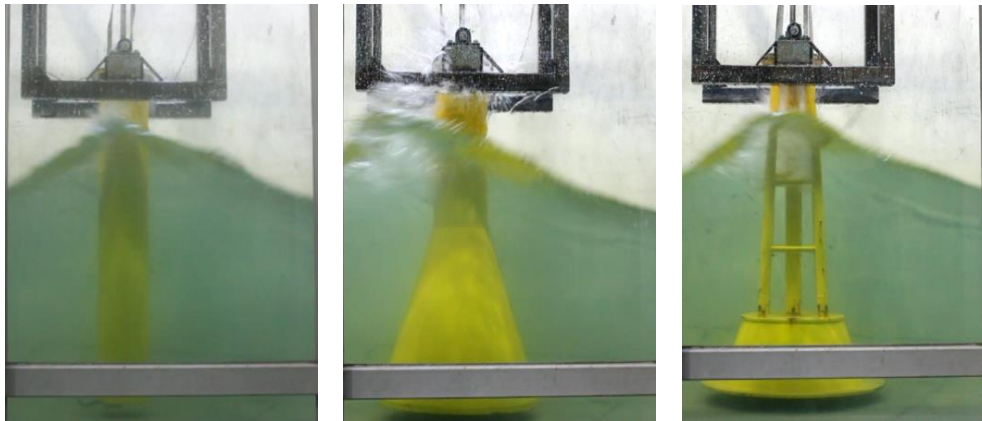
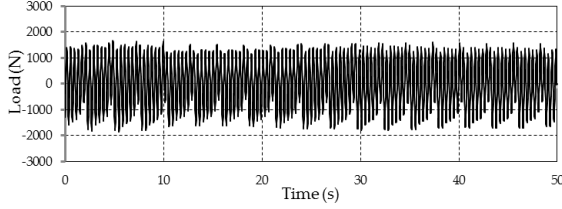(b) Extreme wave condition: Monopile, GBS, Hybrid (1) & (2)
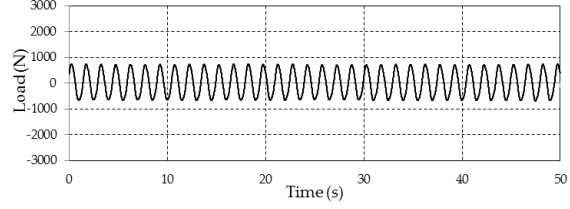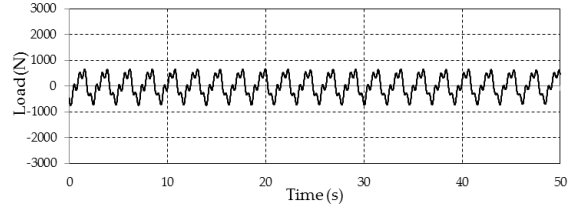
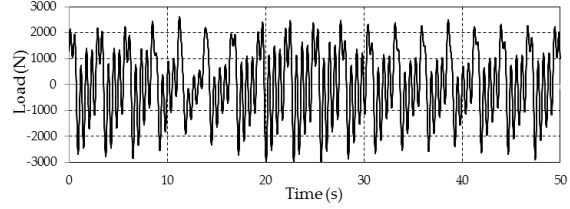Fig. 6 Wave force tests

(a) Wave #1

(a) Wave #1

(b) Wave #3

(b) Wave #3

(c) Wave #6

(c) Wave #6

Fig. 7 Measured wave force of Monopile · · · · · · · · · · · · · · Fig. 8 Measured wave force of GBS
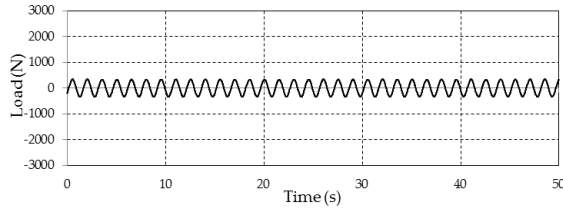
3. Wave forces

3.1 Wave force on regular wave

As the results of wave force tests on the regular wave, measured wave forces for the small-scale models were presented in Fig. 7 to Fig. 10 for the support structure types, respectively. Amplitudes of wave forces for the real-scale models were summarized in Table 3. Test results of this study indicated a similar tendency with wave force theory. In case of the larger diameter support structures of GBS, wave force has been calculated from diffraction theory (F_M) generally, which is mainly governed by the volume V of the wave body of Eq. (2) (Chella *et al*. 2012, Peng 2014).

$$F = F_D + F_M + F_S = f (\rho_w, C_D, A) + f (\rho_w, C_M, V) + f (\rho_w, C_S, C_b, D, \ldots) \qquad (2)$$

where, F, F_D, F_M, and F_S are the total wave force, drag force, inertia force, and slamming force, respectively. C_D, C_M, C_S, and C_b are the drag coefficients for the wave area A, inertia coefficient for the volume V, slamming force factor, and water particle velocity, respectively.

The wave body volume of the GBS type of this study was about 430% of the Monopile, as indicated in Table 1, and total wave force of GBS type ranged from 374% to 506 % (average 440%) of the Monopile at the normal wave condition of wave #1 to wave #5, as presented in Table 3 and Fig. 11, where total wave force did not effected by wave run-up and impact wave force. In case of the slender support structures of jacket or multipiles, wave force has been calculated from
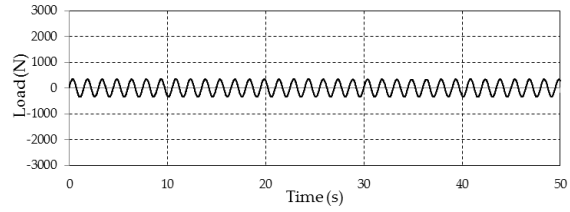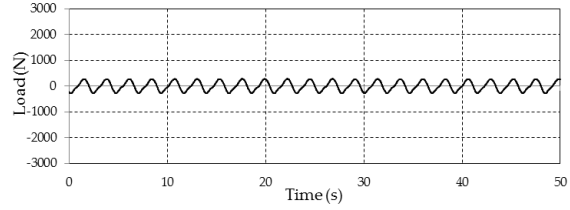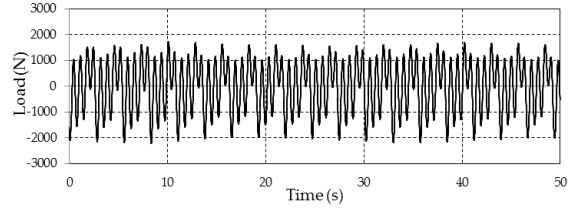
(a) Wave #1
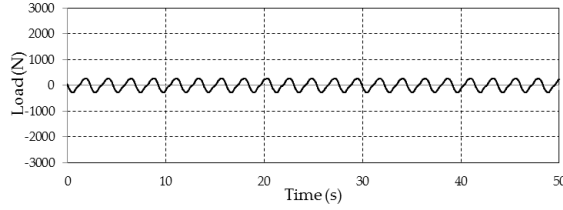
(b) Wave #3
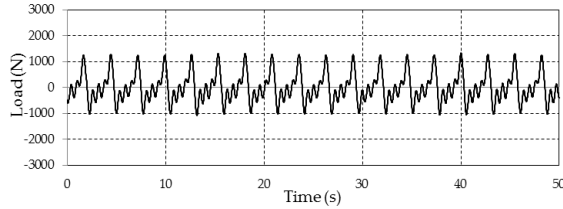
(c) Wave #6

Fig. 9 Measured wave force of Hybrid (1): 0°

(a) Wave #1

(b) Wave #3

(c) Wave #6

Fig. 10 Measured wave force of Hybrid (2): 45°

Morison equation (F_D) generally, which is mainly governed by the area *A* of the wave body of Eq. (2). The wave body areas of the Hybrid (1) and Hybrid (2) of this study were about 180% of the Monopile, as indicated in Table 1, and total wave force of Hybrid (1) and Hybrid (2) ranged from 145% to 203% (average 174%) of the Monopile at the normal wave condition of wave #1 to wave #5, as presented in Table 3 and Fig. 11. Therefore, at the normal wave condition, it was found that wave forces of Hybrid (1) and Hybrid (2) followed theoretical wave area ratio since wave force did not effected by wave run-up and impact wave force. Namely, Hybrid type indicated higher wave force than the Monopile because of the larger wave area of wave body.

At the normal wave condition of wave #1 to wave #5, measured wave force had a similar tendency that, as the wave period increased from wave #1 (7.5 s) to wave #5 (15.5 s) maintaining the same wave height of 3.435 m, wave forces subjected to the support structure decreased for the most support structures, as presented in Fig. 12 (Part *et al*. 2014, 2015). In cases of the Monopile and GBS, wave forces at the long wave period of 15.5 s were about 48.0 % and 55.0 % level, respectively, of the short wave period of 7.5 s. In cases of the Hybrid (1) and Hybrid (2), wave forces at the long wave period of 15.5 s were about 61.0 % and 56.0% level, respectively, of the short wave period of 7.5 s. Hybrid (1) and Hybrid (2), which had the same dimension but different total weight, had the similar wave force level at the normal wave condition of wave #1 to wave #5. Therefore, it was found that total weight of the support structure insignificantly influenced on the wave force subjected to the support structures at the normal wave condition.

At the extreme wave condition of wave #6, measured wave force had a different tendency that, as the wave height increased from wave #4 (3.435 m) to wave #6 (12.78 m) maintaining the same

Table 3 Summary of maximum wave forces for real-scale models

| Sea state		Wave		Monopile	GBS	Hybrid (1)		Hybrid (2)	
						0°	45°	0°	45°
Regular	Normal	#1	Max.	1,064	3,978	1,573	1,539	1,604	1,633
			Ratio	(100 %)	(374 %)	(148 %)	(145 %)	(151 %)	(153 %)
		#2	Max.	793	3,637	1,487	1,446	1,398	1,408
			Ratio	(100 %)	(459 %)	(188 %)	(182 %)	(176 %)	(178 %)
		#3	Max.	759	3,838	1,264	1,266	1,280	1,295
			Ratio	(100 %)	(506 %)	(167 %)	(167 %)	(169 %)	(171 %)
		#4	Max.	605	2,636	1,100	1,093	1,227	1,230
			Ratio	(100 %)	(436 %)	(182 %)	(181 %)	(203 %)	(203 %)
		#5	Max.	511	2,186	954	937	910	908
			Ratio	(100 %)	(428 %)	(187 %)	(183 %)	(178 %)	(178 %)
	Extreme	#6	Max.	10,590	15,481	4,786	4,623	7,802	8,441
			Ratio	(100 %)	(146 %)	(45 %)	(44 %)	(74 %)	(80 %)
Irregular		#7	Max.	1,501	5,763	1,905	1,832	1,876	2,084
			Ratio	(100 %)	(384 %)	(127 %)	(122 %)	(125 %)	(139 %)
		#8	Max.	1,391	4,077	1,811	1,910	1,677	1,622
			Ratio	(100 %)	(293 %)	(130 %)	(137 %)	(121 %)	(117 %)
		#9	Max.	919	3,929	1,492	1,489	1,956	1,444
			Ratio	(100 %)	(428 %)	(162 %)	(162 %)	(213 %)	(157 %)
		#10	Max.	2,125	7,039	3,032	3,650	2,525	2,592
			Ratio	(100 %)	(331 %)	(143 %)	(172 %)	(119 %)	(122 %)
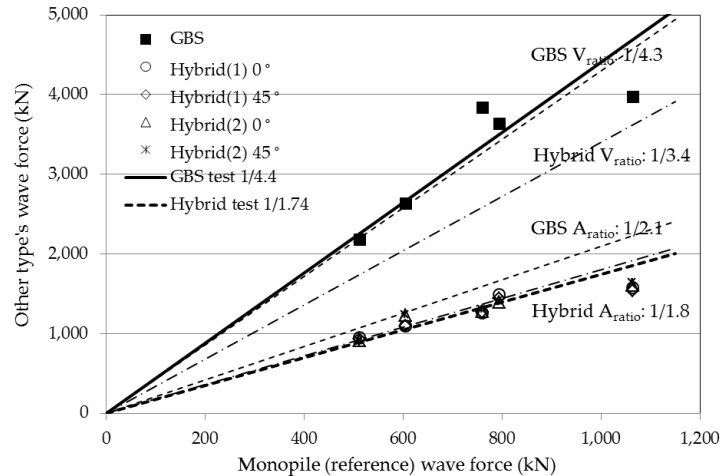
Fig. 11 Wave force ratio to area & volume ratio of wave body on regular wave

wave period of 13.5 s, wave forces subjected to the support structures drastically increased for the most test models although considering effects of the wave height increment, as presented in Fig. 13 and Table 4. In cases of the Monopile and GBS, wave forces at the extreme wave height of
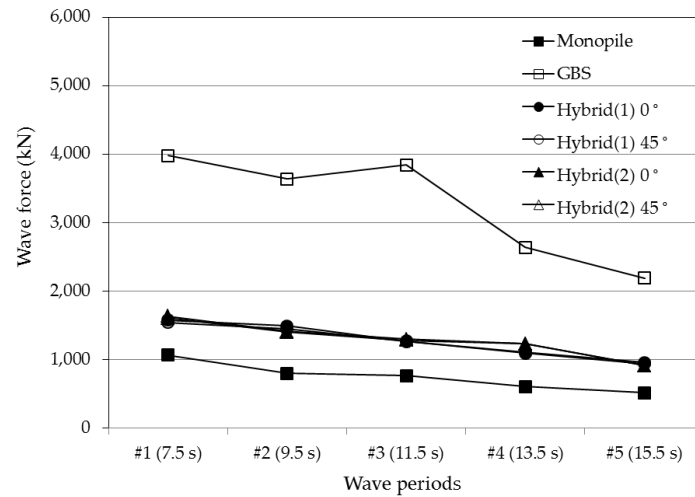
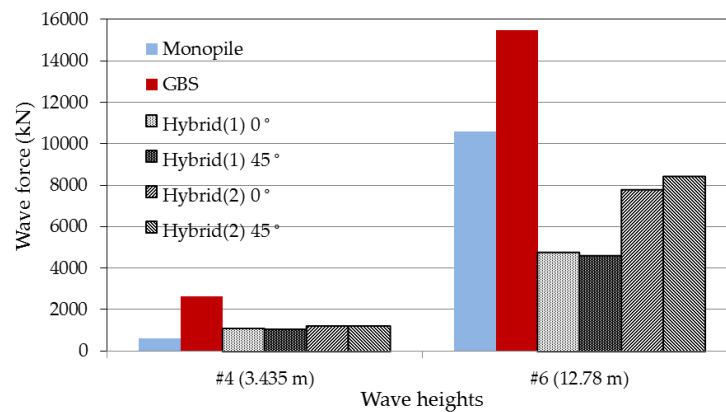Fig. 12 Wave forces to wave periods at normal wave condition

Fig. 13 Wave forces to wave heights at extreme wave condition

Table 4 Wave impact force effects at extreme wave condition

Wave No.	Monopile	GBS	Hybrid (1)		Hybrid (2)	
			0°	45°	0°	45°
#4 (3.435 m)	605	2,636	1,100	1,093	1,227	1,230
#6 (12.78 m)	10,590	15,481	4,786	4,623	7,802	8,441
Ratio (373%)	1,750 %	587 %	435 %	423 %	636 %	686 %

12.78 m were about 1,750 % and 587 % level, respectively, of the normal wave height of 3.435 m. In cases of the Hybrid (1) and Hybrid (2), wave forces at the extreme wave height of 12.78 m were about 423 % to 435 % and 636 % to 686 % level, respectively, of the normal wave height of 3.435 m.

What the extreme wave force of Monopile increased drastically caused by impact wave force called slamming force at the extreme wave condition. According to the study of Christensen *et al.*

Table 5 Wave impact force factors (Chella *et al*. 2012)

References	Impact factor	Type
DNV-OS-J101, DNV-RP-C205	5.15 per unit length	Vertical cylinder
API RP 2A-WSD	0.5π to 1.7 per unit length	
Ros (Ros 2011)	4.3 (test result)	Monopile
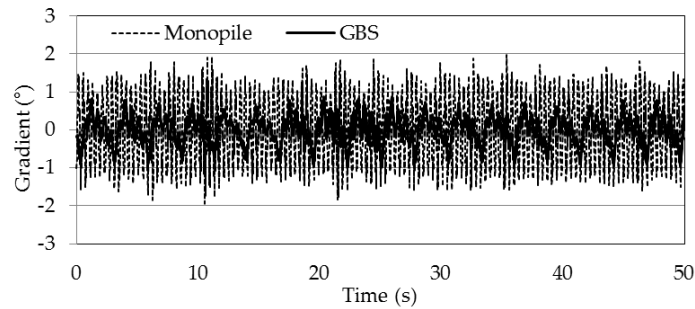
(a) Monopile and GBS
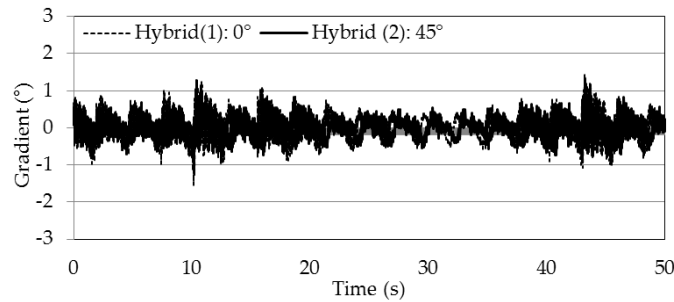
(b) Hybrid (1) and Hybrid (2)

Fig. 14 Wave-induced vibration at the extreme wave #6

(2005), the wave run-up seems to have a maximum for wave height ratio to water depth (H_w/h) 0.67 to 0.80. The wave height ratio to water depth of wave #6 of this study was about 0.64. Considering this wave condition for the wave run-up, the largest impact wave forces were subjected to the test models at wave #6. It has known that the wave run-up and impact wave force was mainly dependent on the shape of support structure, wave height, and wave periods (Christensen *et al*. 2005, De Vos *et al*. 2007, Chella *et al*. 2012). As considering wave height ratio (373%) of wave #6 to wave #4 and slamming force factors (4.3 to 5.15) for the cylinder Monopile, as indicated in Table 5, impact wave force affect largely on the total wave force of the Monopile (Marino *et al*. 2011). Also, wave-induced little vibration of test modes were observed at the extreme wave condition of wave #6, as presented in Fig. 14. The maximum gradient of Monopile due to the wave-induced vibration was about ±2°, and GBS, Hybrid (1), and Hybrid (2) were about ±1°, respectively, at the extreme wave condition of wave #6. Therefore, inertia force due to the little vibration of the Monopile models maybe largely effect on the wave force at the extreme wave condition.

It was natural that impact wave force effect was insignificant for the Hybrid (1) and Hybrid (2) models since the upper part consist of slender member of the multiplies. According to the study of
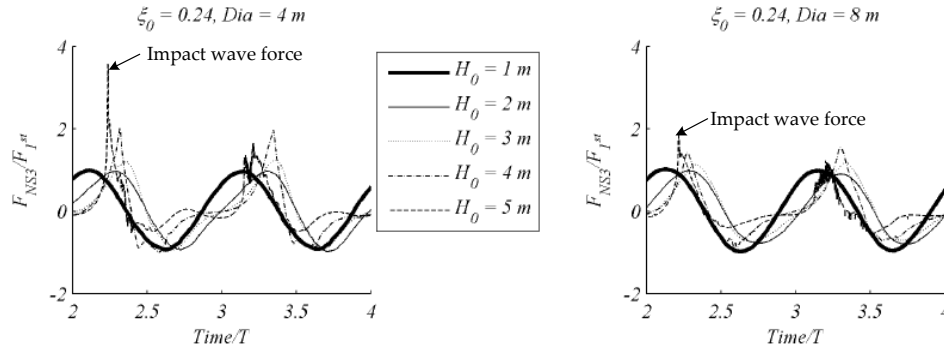
Fig. 15 Extreme wave force to the wave height and diameter of support structure (Christensen *et al.* 2005)

Aashamar (2012), it was found to get significantly lower wave slamming forces on truss structure members than on a monopile. However, it was a question that the impact wave force effect of GBS type was minute. According to the other theoretical study (Christensen *et al.* 2005), as the diameter of the support structure increased within a certain range, it was found that impact wave force degreased in rather, as presented in Fig. 15, where H_0 and T were the wave height (H_w) and wave periods (P_w), respectively. ξ_0 was the surf similarity parameter defined as $\xi_0 = \tan(\beta) / \sqrt{H_0/L_0}$, where β was the seabed slope given in degree and L_o was the wave length (L_w), respectively. Therefore, impact wave force effect of this study for the GBS type was reasonable.

Hybrid (1) and Hybrid (2), which had the same dimension but different total weight, were indicated different levels of the wave force at the extreme wave condition of wave #6. It was caused by different inertia force due to the wave-induced little vibration of the test models at the extreme wave condition. Wave forces of GBS type indicated the largest wave force among the four support structures, about 374% to 506% of the Monopile at the normal wave condition of wave #1 to wave #5 and about 146% at the extreme wave condition of wave #6. At the extreme wave condition of wave #6, wave forces of Hybrid (1) and Hybrid (2) indicated about 44% to 45%, and 74% to 80% of the Monopile, respectively, as indicated in Table 3, although wave force of Hybrid (1) and Hybrid (2) indicated about 182% to 203% at the normal wave condition of wave #4.

Summarizing wave force test results on the regular wave, as the wave period increased maintaining the same wave height at the normal wave condition, wave force subjected to the support structures decreased for the most support structures. Also, total weights of the support structures insignificantly influenced on the wave force subjected to the support structure at the normal wave condition. As the wave height increased maintaining the same wave period at the extreme wave condition, wave force subjected to the support structures influenced by impact wave force called slamming force. Wave run-up and impact wave force were mainly dependent on the shape of substructure, wave height, and wave period. Impact wave force of this study significantly effect on the Monopile and slightly to the other models. Also, wave-induced little vibration of the test models at the extreme wave condition, against to the normal wave condition, influenced on the wave force subjected to the support structure causing different inertia force.
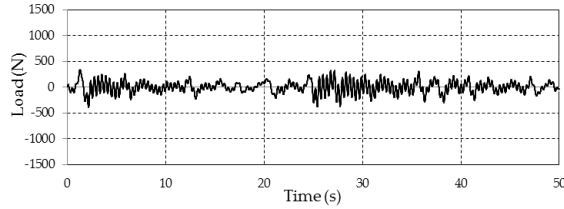
In respects of the structural design, critical loading is wave force at the extreme wave condition rather than the normal wave condition. Hybrid (1) and Hybrid (2) had a larger wave projection area about 180% of the Monopile, as indicated in Table 1. Therefore, Hybrid (1) and Hybrid (2)
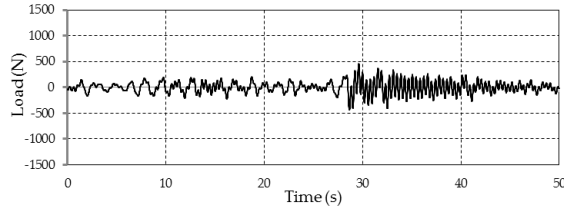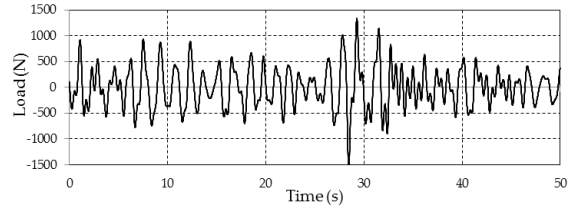
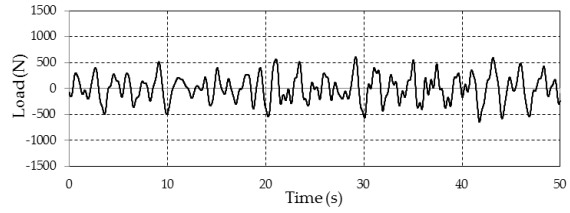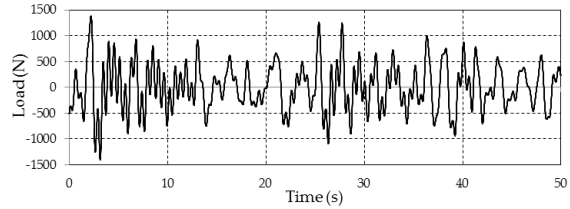(a) Wave #7
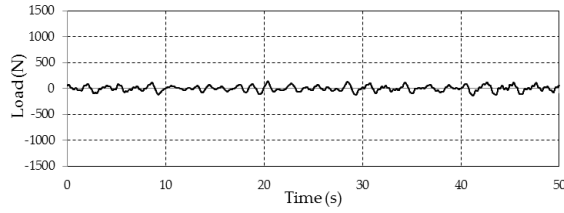
(b) Wave #9

(c) Wave #10

Fig. 16 Measured wave force of Monopile
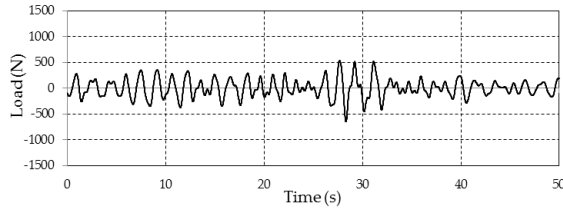

(a) Wave #7

(b) Wave #9

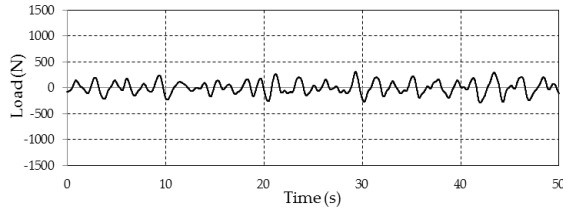(c) Wave #10

Fig. 17 Measured wave force of GBS

indicated higher wave forces about 145% to 203% (average 174%) of the Monopile at the normal wave condition of wave #1 to wave #5. However, at the extreme wave condition of wave #6, Hybrid (1) and Hybrid (2) indicated lower wave forces about 44% to 80% (average 60.7%) levels of the Monopile. It was caused by lower wave run-up and impact wave force according to the fluid-multipile interaction, since the upper part of Hybrid (1) and Hybrid (2) consist of the slender multipile member which was advantage to reduce wave run-up and impact wave force at the extreme wave conditions.
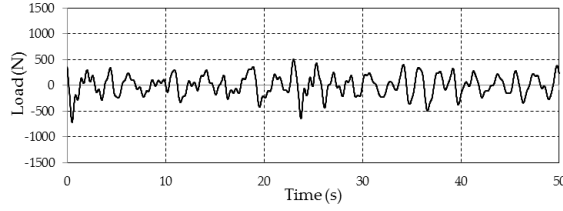
3.2 Wave force on irregular wave

As the results of wave force tests on the irregular wave, measured wave forces for the small-scale models were presented in Fig. 16 to Fig. 19 for the support structure types, respectively. Also, amplitudes of wave forces for the real-scale models were summarized in Table 3. Test results on the irregular waves of this study underestimated with the wave force theory, as presented in Fig. 20. The wave body volume of the GBS type was about 430% of the Monopile, as indicated in Table 1, and total wave force of GBS type ranged from 293% to 428% (average 359%) of the Monopile at the irregular wave condition of wave #7 to wave #10, as presented in Table 3 and Fig. 20. The wave body areas of the Hybrid (1) and Hybrid (2) were about 180% of the Monopile, as indicated in Table 1, and total wave force of Hybrid (1) and Hybrid (2) ranged from 117% to 213% (average 142%) of the Monopile at the irregular wave condition of wave #7 to wave #10, as presented in Table 3 and Fig. 20. Irregular wave conditions included the extreme wave as well as
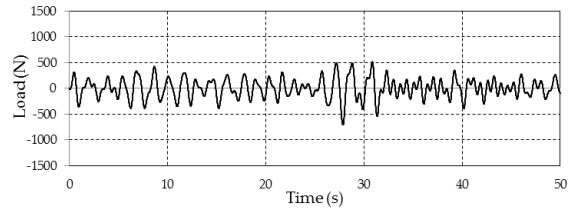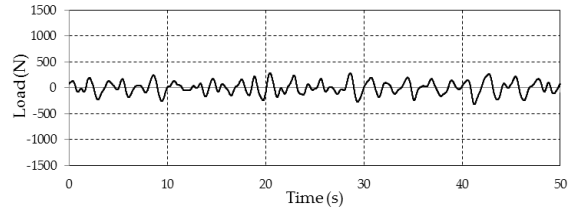
Fig. 18 Measured wave force of Hybrid (1): 0°
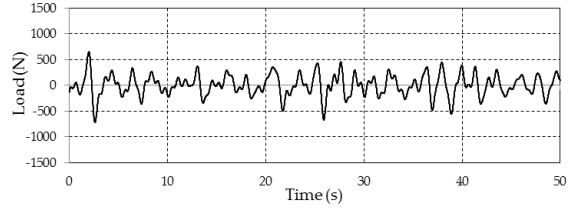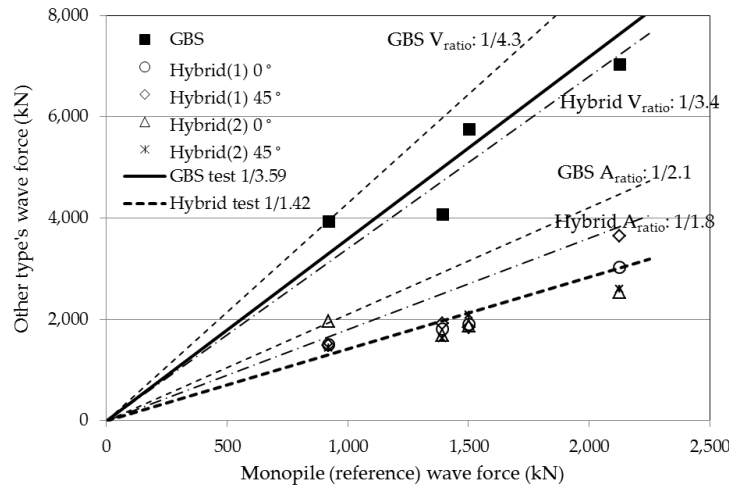

Fig. 19 Measured wave force of Hybrid (2):45°

Fig. 20 Wave force ratio to area & volume ratio of wave body on irregular wave

the normal wave with JONSWAP spectrum. Therefore, some of the higher impact wave force terms for the Monopile at the extreme wave conditions, as illustrated in section 3.1, were reflected at the wave force of the Monopile on irregular wave conditions. Therefore, wave forces of the GBS, Hybrid (1), and Hybrid (2) models on the irregular wave condition were indicated relatively lower wave forces than the Monopile.
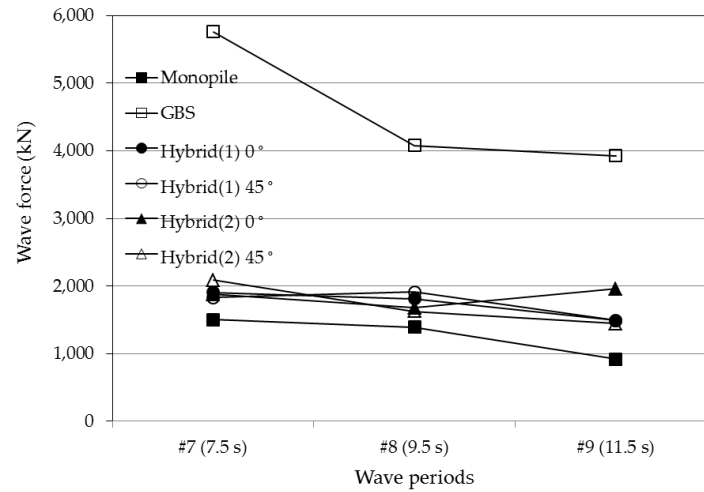
Fig. 21 Wave forces to wave periods at normal wave condition

At the irregular wave condition of wave #7 to wave #9, measured wave force had a similar tendency that, as the wave period increased from wave #7 (7.5 s) to wave #9 (11.5 s) maintaining the same wave height of 3.435 m, wave forces subjected to the support structure decreased for the most support structures, as presented in Fig. 21. In cases of the Monopile and GBS, wave forces at the long wave period of 11.5 s were about 61.2 % and 68.2 % level, respectively, of the short wave period of 7.5 s. In cases of the Hybrid (1) and Hybrid (2), wave forces at the long wave period of 11.5 s were about 74.8 % and 86.8 % level, respectively, of the short wave period of 7.5 s. Hybrid (1) and Hybrid (2), which had the same dimension but different total weight, had the similar wave force level on the irregular wave condition of wave #7 to wave #9.

Summarizing wave force test results on the irregular wave, as the wave period increased maintaining the same wave height, wave force subjected to the support structures decreased for the most support structures. Also, total weights of the support structures insignificantly influenced on the wave force subjected to the support structure at the irregular wave condition. Wave forces of the GBS, Hybrid (1), and Hybrid (2) models on the irregular wave condition were indicated relatively lower wave forces than the Monopile, since some of the higher impact wave force terms for the Monopile at the extreme wave conditions was reflected at the wave force of the Monopile on irregular wave conditions.

4. Conclusions

In this study, wave force tests were carried out for the four types of offshore support structures, Monopile, GBS (Gravity Base System), Hybrid (1), and Hybrid (2). Based on the wave force tests, wave forces to the shapes of the support structures were analyzed and compared with each other.

As the results of this study, it was found that, as the wave period increased maintaining the same wave height at the normal and irregular wave condition, wave force subjected to the support structure decreased for the most cases. As the wave height increased maintaining the same wave period at the extreme wave condition, wave force subjected to the support structure influenced by

impact wave force called slamming force. Although impact wave force of this study significantly effect on the Monopile, since the impact wave force has nonlinearity and complication dependent on the support structure shape, wave height, and wave period, more research is needed to access the impact wave force for other support structure shapes and wave conditions.

Wave forces from wave force test of this study had a good agreement with the wave force theory at the normal wave condition of regular wave. However, wave forces of the GBS and Hybrid models on the irregular wave condition were indicated relatively lower wave forces terms than the Monopile since some of the higher impact wave force for the Monopile at the extreme wave conditions was reflected at the wave force of the Monopile on irregular wave conditions.

In respects of the structural design, critical loading is wave force at the extreme wave condition rather than the normal wave condition. Although Hybrid (1) and Hybrid (2) models had a larger wave projection area than the Monopile, Hybrid (1) and Hybrid (2) models indicated lower wave forces than the Monopile at the extreme wave condition resulting from lower impact wave force effects. Therefore, it was expected that the Hybrid model of this study contribute to improve structural safety of offshore support structure as decreasing wave force at the extreme wave conditions.

Acknowledgments

References

Aashamar, M.Z. (2012), "Wave slamming forces on truss support structures for wind turbines", Master Thesis, Norwegian University of Science and Technology, Trondheim, Norway.

Brook-Hart, W., Jakson, P.A., Meyts, M. and Gifford, P. (2010), "Competitive concrete foundations for offshore wind turbines", *International Foundation*.

Cao, D., Yat-Man, E.L., Jian, W. and Huang, Z. (2016), "An experimental study of wave runup: cylinder fixed in waves versus cylinder surging in still water", ICCOE 2016-C1002, Tokyo, Japan.

Chella, M.A., Torum, A. and Myrhaug, D. (2012), "An overview of wave impact forces on offshore wind turbine substructures", *Energy Procedia*, **20**, 217-226.

Christensen, E.D., Bredmose, H. and Hansen, E.A. (2005), "Extreme wave forces and wave run-up on offshore wind turbine foundations", *Proceedings of Copenhagen Offshore Wind Conference*, 1-10.

De Vos, L., Frigaard, P. and Rouck, J.D. (2007), "Wave run-up on cylindrical and cone shaped foundations for offshore wind turbines", *Coastal Eng.*, **54**(1), 17-29.

DNV (2013), Offshore Standard DNV-OS-J101: Design of Offshore Wind Turbine Structures, Det Norske Veritas AS, Norway.

Fischer, T., De Vries, W. and Schmidt, B. (2010), *Upwind Design Basis (WP4: Offshore Foundations and Support Structures)*, Upwind.

Jeong, Y.J., Park, M.S. and You, Y.J. (2015), "Shape dependent wave force and bending moment of offshore wind substructure system", *Int. J. Constr. Res. Civil Eng.*, **1**(2), 16-26.

Jeong, Y.J., You, Y.J., Park, M.S., Lee, D.H. and Kim, B.C. (2013), "Structural safety and design requirements of CFMP based offshore wind substructure system", OCEANS 2013-130505, Virginia, USA.

Jeong, Y.J., You, Y.J., Park, M.S., Lee, D.H. and Kim, B.C. (2014), "CFMP based offshore wind substructure system and modular installation method", *EWEA 2014-130505*, Barcelona, Spain.

Marino, E., Borri, C. and Peil, U. (2011), "A fully nonlinear wave model to account for breaking wave impact loads on offshore wind turbines", *J. Wind Eng. Indus. Aerodyn.*, **99**, 483-490.

NEDO (2013), *NEDO Offshore Wind Energy Progress*, NEDO 2013, Japan.

Park, M.S., Jeong, Y.J., You, Y.J. and Lee, D.H. (2015), "Numerical analysis of a gravity substructure with suction bucket foundation for 5MW offshore wind turbine", *Offshore Technology; Offshore Geotechnics*, St. John's, Newfoundland, Canada, May-June.

Park, M.S., Jeong, Y.J., You, Y.J., Lee, D.H. and Kim, B.C. (2014), "Numerical analysis of a hybrid substructure for offshore wind turbine", *Ocean Syst. Eng.*, **4**(3), 169-183.

Park, M.S., Koo, W.C. and Choi, Y.R. (2010), "Hydrodynamic interaction with an array of porous circular cylinders", *Int. J. Naval Arch. Ocean Eng.*, **2**(3), 146-154.

Park, M.S., Koo, W.C. and Kawana, K. (2012), "Numerical analysis of the dynamic response of an offshore platform with a pile-soil foundation system subjected to random waves and currents", *J. Waterw. Port, Coast. Ocean Eng.*,ASCE, **138**(4), 275-285.

Peng, Z. (2014), "Wave slamming impact on offshore wind turbine foundations", *Coastal Engineering Conference*, **1**(34), 43..

Rockmat (2013), Foundation for Rocky Seabeds, www.youtube.com/watchtv=-gToiG2OFOI, 2013.

Ros, X. (2011), "Impact forces on a vertical pile from plunging breaking waves", Master Thesis, Norwegian University of Science and Technology, Department of Civil and Transport Engineering, Trondheim, Norway.

PL